Theoret. Chim. Acta (Berl.) 50, 95–116 (1978)

THEORETICA CHIMICA ACTA

Original Investigations

Crystal Field Calculation of g Values and Zero-Field Splitting for High Spin Ferric Complexes of Rhombic Character

Amy S. Rispin, Mitsuo Sato* and Hideo Kon

Laboratory of Chemical Physics, National Institute of Arthritis, Metabolism and Digestive Diseases, National Institutes of Health, Bethesda, Maryland 20014, USA

For high spin ferric ions in rhombic symmetry, we have used a crystal field model to relate term splittings of the $^4T_1$, $^2T_2$ and $^4T_2$ excited states to zero-field split energies and g values of the $^6A_1$ term. In this model five crystal field parameters were used, namely, one cubic parameter, two tetragonal parameters and second and fourth order rhombic parameters. In tetragonal symmetry with only three crystal field parameters, a simpler model including only the $^4T_1$ and $^2T_2$ excited states is adequate to relate term energies to g values and zero-field split energies. However, we have demonstrated the importance of the $^4T_2$ state in rhombic crystalline fields. No higher lying terms other than $^4T_2$ can influence the $^4T_1$ term directly through the tetragonal or rhombic crystal field. Furthermore, we show that the fourth order rhombic crystal field parameter is a key parameter because the rhombic splitting of the dominant low lying $^4T_1$ term of high spin ferric complexes depends to first order on the fourth order crystal field potential. We have performed a computer diagonalization of the spin-orbit, electrostatic and crystal field perturbation matrix, and calculated g values and zero-field splittings in seventeen high spin ferric mixed crystalline species of varying rhombicities and for metmyoglobin and cytochrome P-450. The high spin and spin-mixed regions are developed completely to yield the crystal field term energies, zero-field splittings and basis functions together with g values.

Key words: High spin ferric complexes – Zero field splitting – Rhombicity

*Present address: Faculty of Pharmaceutical Sciences, Teikyo University, Sagamiko-cho, Kanagawa 199-01, Japan.

0040–5744/78/0050/0095/$04,40

1. Introduction

Investigations of magnetic properties of the active sites of heme proteins such as cytochrome P-450 or metmyoglobin can lead to insight into their structure. Rhombicity observed in EPR of some ferric heme proteins may be a result of bonding of iron to an asymmetric axial ligand such as cysteine or imidazole and/or geometric distortion of the heme portion of the protein [1]. The ratio E/D is a measure of rhombicity and can be obtained from g values by means of the spin Hamiltonian formalism. Crystal field calculations can provide a unifying theory to relate separate values of E and D to measured g values and zero-field splittings. In addition, one-electron energy levels can be determined for a given rhombicity and excited state term energies can be related to ground state energy splittings. Furthermore, by means of crystal field calculations, trends in g values from compound to compound and within one compound as ligands or heme geometries change, can be related to variation in crystal field parameters and degree of spin mixing.

Crystal field calculations of zero-field splittings, g values and other magnetic properties of ferric porphyrins in tetragonal symmetry have been done by Harris [2] and by Otsuka [3]. Harris used a strong field treatment in which the $^6A_1$ ground state and $^4T_1$ and $^2T_2$ excited state perturbation matrices were diagonalized.

Eicher [4] has done a weak crystal field calculation of slightly rhombic ferric porphyrins (metmyoglobins and methemoglobin) in which he included every excited state arising from the d^5 weak-field configuration. In this calculation, crystal field parameter fittings were facilitated by correlation with experimental results for high spin ferrous compounds.

Previously we have made a complete spin Hamiltonian analysis of highly rhombic ferric heme compounds including quartic as well as quadratic zero-field terms and carrying out the perturbation calculation of Zeeman interaction to third order [5]. This analysis was made possible by measurements of a series of model compounds (mixed crystals, $TPPH_2(FeX)$) with E/D varying from slightly rhombic (comparable to metmyoglobin) to highly rhombic (similar to cytochrome P-450) [6]. In these model compounds, g values were observable for the middle as well as lower Kramers doublets. These data made possible the separate determination of E and D. A crystal field perturbation calculation, using the basis set $^6A_1$, $^4T_1$, $^2T_2$ was made relating the spin Hamiltonian and crystal field parameters so that the crystal field energy scheme could be calculated from observed g values.

We now show that in a highly rhombic system the basis set must be extended to include the $^4T_2$ excited state as well as the $^6A_1$, $^4T_1$ and $^2T_2$ states. The inclusion of this $^4T_2$ state enhances the calculated rhombic splitting of the first excited $^4T_1$ state because the tetragonal and rhombic crystal field potential mixes the $^4T_1$ and $^4T_2$ states directly. This enhanced rhombic splitting is transmitted to the ground state through spin-orbit interaction and affects the zero-field splitting and anisotropy of g values. No higher lying terms other than $^4T_2$ can influence the $^4T_1$ term directly through the tetragonal or rhombic crystal field. Therefore, the set chosen, $^6A_1$, $^4T_1$, $^2T_2$ and $^4T_2$, is necessary and sufficient for strong crystal field treatments of

rhombically distorted heme compounds. To describe the effect of the $^4T_2$ term accurately by the perturbation method would require that the order of the perturbation be carried prohibitively far because the off-diagonal matrix elements of the tetragonal and rhombic crystal field may be of the same order of magnitude as the energy differences involved. Therefore we have performed a computer diagonalization of the spin-orbit, electrostatic and rhombic crystal field energy matrix, and calculated g values and zero-field splittings in seventeen high spin ferric mixed crystalline species ($TPPH_2(FeX)$) of varying rhombicities and for metmyoglobin and cytochrome P-450. Although by such a computer diagonalization one loses the clarity of the analytical relationship from the spin Hamiltonian to the crystal field parameters, the high spin and spin-mixed regions can be developed completely to yield the crystal field term energies, zero-field splittings and basis functions together with g values. (An exploration of low spin and spin-mixing regions in rhombic ferric heme proteins is in progress.)

An algorithm is used which enables the spin Hamiltonian parameters to be related to the crystal field parameters in the limited basis set. The theory is then extended to include the extra $^4T_2$ term in rhombic symmetry. We will show that the fourth order rhombic crystal field parameter, A_{42} is a key parameter for rhombic heme compounds because the rhombic splitting of the dominant low lying $^4T_1$ term of high spin ferric complexes depends to first order on the fourth order crystal field potential, $Y_{4\pm2}$.

2. Theoretical Formulation

The complete crystal field Hamiltonian used has cubic, tetragonal and rhombic contributions. After collecting coefficients A_{LM} of like order in the spherical harmonics, Y_{LM}, the crystal field potential is

$$V_{\text{C.F.}} = A_{40}(r^4)Y_{40} + A_{44}(r^4)[Y_{44} + Y_{4-4}] + A_{20}(r^2)Y_{20} + A_{22}(r^2)[Y_{22} + Y_{2-2}] + A_{42}(r^4)[Y_{42} + Y_{4-2}] \tag{1}$$

The first three terms are octahedral and tetragonal contributions combined, and the last two denote rhombic distortion. One-electron crystal field energies are shown in Fig. 1 and given here in terms of crystal field parameters.

$$\begin{aligned}
\Delta &= \frac{7}{6}\frac{5}{14\sqrt{\pi}}A_{40} + \frac{5}{6}\sqrt{\frac{5}{14\pi}}A_{44} \\
\delta' &= \frac{-2}{7}\sqrt{\frac{5}{\pi}}A_{20} - \frac{5}{14\sqrt{\pi}}A_{40} + \sqrt{\frac{5}{14\pi}}A_{44} \\
\delta &= \frac{3}{14}\sqrt{\frac{5}{\pi}}A_{20} - \frac{5}{15\sqrt{\pi}}A_{40} + \sqrt{\frac{5}{14\pi}}A_{44} \\
\mu' &= \frac{-2}{7}\sqrt{\frac{10}{\pi}}A_{22} + \frac{2}{7}\sqrt{\frac{15}{2\pi}}A_{42} \\
\mu &= \frac{2}{7}\sqrt{\frac{15}{2\pi}}A_{22} + \frac{2}{7}\sqrt{\frac{10}{\pi}}A_{42}
\end{aligned} \tag{2}$$

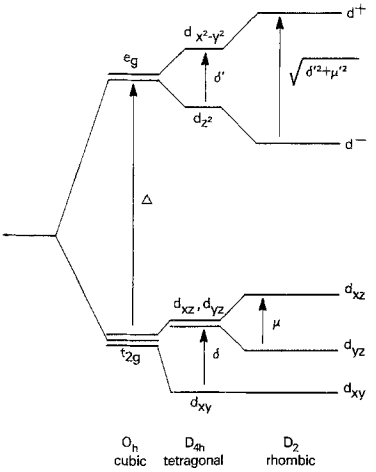

Fig. 1. One-electron energy splittings

The one-electron rhombic splittings are determined by μ' and μ which are functions of both the second and fourth order rhombic parameters, A_{22} and A_{42}. For the sake of comparison with Harris [2], we relate the crystal field parameters to a set of new parameters in terms of which we will express the term splittings:

$$\begin{aligned} \Delta_{\mathrm{Oh}} &= 2\sqrt{\frac{5}{14\pi}}\,A_{44} \\ U' &= \frac{-4}{14}\sqrt{\frac{5}{\pi}}\,A_{20} \\ C' &= \sqrt{\frac{5}{14\pi}}\,A_{44} - \frac{5}{14\sqrt{\pi}}\,A_{40} \end{aligned} \tag{3}$$

Then, the one-electron splittings Δ, δ and δ' can be expressed in terms of the terms splitting parameters Δ_{Oh}, C' and U':

$$\begin{aligned} \delta &= \frac{-3}{4}\,U' + C' \\ \delta' &= U' + C' \\ \Delta &= \Delta_{\mathrm{Oh}} - \tfrac{7}{6}C' \end{aligned} \tag{4}$$

Or,

$$\begin{aligned} C' &= \tfrac{3}{7}\delta' + \tfrac{4}{7}\delta \\ \Delta_{\mathrm{Oh}} &= \Delta + \tfrac{1}{2}\delta' + \tfrac{2}{3}\delta \\ U' &= \tfrac{4}{7}(\delta' - \delta) \end{aligned} \tag{5}$$

Δ_{Oh} represents the true octahedral crystal field component, C' and U' the tetragonal crystal field. We use the coefficients A_{42} and A_{22} to denote the rhombic distortion.

$$A_{22} = \sqrt{\frac{2\pi}{5}}\left(\frac{\sqrt{3}}{2}\mu - \mu'\right)$$
$$A_{42} = \sqrt{\frac{2\pi}{5}}\left(\mu + \frac{\sqrt{3}}{2}\mu'\right) \tag{6}$$

Convenience of fitting g values dictates that we vary the parameters that are simply related to term splittings. These parameters are Δ_{Oh}, C' and U' in the tetragonal limit and, as we show below, A_{22} and A_{42} in the presence of rhombic distortion.

In the high spin d^5 electron configuration, zero-field splittings and g value anisotropy depend on mixing of the orbitally non-degenerate $^6A_1$ ground state with excited states of quartet and doublet character through both spin-orbit and crystal field interaction. Particularly important in anisotropy of g values is the mixing of the first excited $^4T_1$ state with the $^6A_1$ state via second order spin-orbit interaction. Rhombic crystal field splitting of the $^4T_1$ state is directly reflected in anisotropy of g values. The $^4T_1$ $(t_{2g}^4 e_g)$ state mixes via spin-orbit interaction with the $^2T_2(t_{2g}^5)$ state and via the tetragonal and rhombic crystal field potentials as well as spin-orbit interaction with the $^4T_2(t_{2g}^4\, e_g)$ state. Moreover, since neither the rhombic nor tetragonal crystal field operators mix e_g with t_{2g} orbitals, only the $^4T_2$ state which is within the same configuration as the $^4T_1$ state, need be considered to first order as an additional term above the $^2T_2$ state in rhombic systems. Any other high lying terms would influence the $^4T_1$ term only indirectly via spin-orbit interaction. Previously, Harris has shown the sufficiency of the basis $^6A_1$, $^4T_1$, $^2T_2$ in the tetragonal limit of high spin term compounds [2]. But tetragonal and rhombic crystal field mixing of the $^4T_2$ state with the $^4T_1$ state enhances the anisotropy of g values strongly as rhombicity increases. Inclusion of the $^4T_2$ state also increases the zero-field splitting energies slightly.

Using the $^6A_1(t_{2g}^3\, e_g^2)$, $^4T_1(t_{2g}^4\, e_g)$, $^2T_2(t_{2g}^5)$ and $^4T_2(t_{2g}^4\, e_g)$ terms as a basis set, an energy matrix (36×36) was derived containing Racah parameters A, B, and C for term energies [7] and cubic, tetragonal and rhombic crystal field as well as spin-orbit interaction matrix elements.

The method of irreducible tensors and coupling coefficients in point groups using the conventions of Griffith [7] was used to derive a real basis of 5-electron terms.

Electrostatic energies of excited state terms are expressed using Racah parameters.

$$\begin{aligned} E(^6A_1) &= 10A - 35B \\ E(^4T_1) &= 10A - 25B + 6C \\ E(^2T_2) &= 10A - 20B + 10C \\ E(^4T_2) &= 10A - 17B + 6C \end{aligned} \tag{7a}$$

Crystal field matrix elements follow (see Fig. 2):

$$\langle {}^4T_1 z|V_{CF}|{}^4T_1 z\rangle = -\Delta_{\mathrm{Oh}}$$

$$\langle {}^4T_1 x|V_{CF}|{}^4T_1 x\rangle = -\Delta_{\mathrm{Oh}}+\frac{7}{4}C'-\frac{\sqrt{3}}{4}\mu'-\frac{1}{2}\mu$$

$$\langle {}^4T_1 y|V_{CF}|{}^4T_1 y\rangle = -\Delta_{\mathrm{Oh}}+\frac{7}{4}C'+\frac{\sqrt{3}}{4}\mu'+\frac{1}{2}\mu$$

$$\langle {}^2T_2 \xi|V_{CF}|{}^2T_2 \xi\rangle = -2\Delta_{\mathrm{Oh}}+2C'+\frac{1}{4}U'+\frac{1}{2}\mu$$

$$\langle {}^2T_2 \eta|V_{CF}|{}^2T_2 \eta\rangle = -2\Delta_{\mathrm{Oh}}+2C'+\frac{1}{4}U'-\frac{1}{2}\mu$$

$$\langle {}^2T_2 \zeta|V_{CF}|{}^2T_2 \zeta\rangle = -2\Delta_{\mathrm{Oh}}+3C'-\frac{1}{2}U'$$

$$\langle {}^4T_2 \xi|V_{CF}|{}^4T_2 \xi\rangle = -\Delta_{\mathrm{Oh}}+\frac{5}{4}C'-\frac{1}{2}U'+\frac{\sqrt{3}}{4}\mu'-\frac{1}{2}\mu \qquad (7b)$$

$$\langle {}^4T_2 \eta|V_{CF}|{}^4T_2 \eta\rangle = -\Delta_{\mathrm{Oh}}+\frac{5}{4}C'-\frac{1}{2}U'-\frac{\sqrt{3}}{4}\mu'+\frac{1}{2}\mu$$

$$\langle {}^4T_2 \zeta|V_{CF}|{}^4T_2 \zeta\rangle = -\Delta_{\mathrm{Oh}}+C'+U'$$

$$\langle {}^4T_1 z|V_{CF}|{}^4T_2 \zeta\rangle = \frac{1}{2}\mu'$$

$$\langle {}^4T_1 x|V_{CF}|{}^4T_2 \xi\rangle = -\frac{\sqrt{3}}{4}C'-\frac{\sqrt{3}}{4}U'-\frac{1}{4}\mu'$$

$$\langle {}^4T_1 y|V_{CF}|{}^4T_2 \eta\rangle = \frac{\sqrt{3}}{4}C'+\frac{\sqrt{3}}{4}U'-\frac{1}{4}\mu'$$

For five electrons in rhombic symmetry with spin-orbit interaction, each state reduces to the $E_{1/2}$ representation of the D_2' double group. Spin-orbit matrix elements are given within one basis set of the time-reversal pair in Table 1. One-electron spin-orbit interaction operators were used. Reduction to D_2' symmetry and derivation of Kramers doublet time-reversal pairs was based on original methods by one of the authors [8]. One-electron time-reversal operators were after Tanabe, Sugano and Kamimura [9]. Since the crystal field and spin-orbit interaction operators do not mix time-reversal pairs, the total energy matrix is block diagonalized into two 18×18 matrices.

When diagonalized, this matrix gives eigenvalues and hence the zero-field splittings essentially to complete order of perturbation within the basis set. The eigenvectors are obtained as linear combinations of 5-electron states. The eigenvectors corresponding to the three lowest doubly degenerate eigenvalues then constitute the three Kramers doublets of the ground state. These Kramers doublet eigenvectors

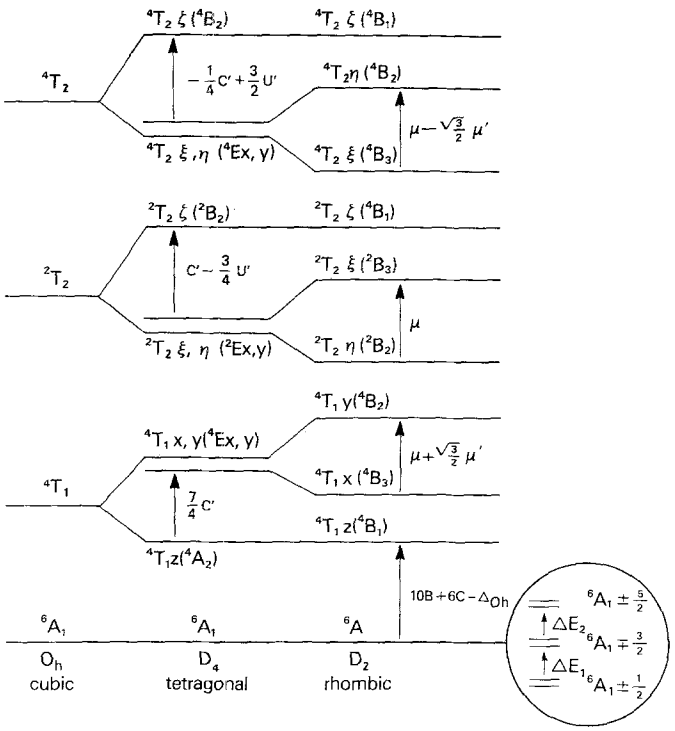

Fig. 2. Term splittings

Table 1. Spin-orbit interaction matrix elements within a time-reversal set in terms of the spin-orbit parameter

	$^4T_1x\ 3/2$	$^4T_1y\ 3/2$	$^4T_1z\ 1/2$	$^4T_1x\ -1/2$	$^4T_1y\ -1/2$	$^4T_1z\ -3/2$
$^6A_1\ 5/2$	$-i$	-1	0	0	0	0
$^6A_1\ 1/2$	$i/\sqrt{10}$	$-1/\sqrt{10}$	$-i\sqrt{6/5}$	$-i\sqrt{3/10}$	$-\sqrt{3/10}$	0
$^6A_1\ -3/2$	0	0	0	$i\sqrt{3/5}$	$-\sqrt{3/5}$	$i2/\sqrt{5}$
$^4T_1x\ 3/2$	0	$i/4$	$-1/4\sqrt{3}$	0	0	0
$^4T_1y\ 3/2$	$-i/4$	0	$i/4\sqrt{3}$	0	0	0
$^4T_1z\ 1/2$	$-1/4\sqrt{3}$	$-i/4\sqrt{3}$	0	1/6	$-i/6$	0
$^4T_1x\ -1/2$	0	0	1/6	0	$-i/12$	$-1/4\sqrt{3}$
$^4T_1y\ -1/2$	0	0	$i/6$	$i/12$	0	$i/4\sqrt{3}$
$^4T_1z\ -3/2$	0	0	0	$-1/4\sqrt{3}$	$-i/4\sqrt{3}$	0
$^2T_2\zeta\ 1/2$	$-\sqrt{3}/2$	$\sqrt{3}\ i/2$	0	$-1/2$	$-i/2$	0
$^2T_2\xi\ -1/2$	0	0	$-1/2$	0	$-i$	$-\sqrt{3}/2$
$^2T_2\eta\ -1/2$	0	0	$i/2$	$-i$	0	$-\sqrt{3}\ i/2$
$^4T_2\xi\ 3/2$	0	$-i\sqrt{3}/4$	$-1/4$	0	0	0
$^4T_2\eta\ 3/2$	$-i\sqrt{3}/4$	0	$-i/4$	0	0	0
$^4T_2\zeta\ 1/2$	1/4	$-i/4$	0	$-1/2\sqrt{3}$	$-i/2\sqrt{3}$	0
$^4T_2\xi\ -1/2$	0	0	$1/2\sqrt{3}$	0	$i/4\sqrt{3}$	$-1/4$
$^4T_2\eta\ -1/2$	0	0	$-i/2\sqrt{3}$	$i/4\sqrt{3}$	0	$-i/4$
$^4T_2\zeta\ -3/2$	0	0	0	1/4	$-i/4$	0

Table 1.—*continued*

	$^4T_2\xi$ 3/2	$^4T_2\eta$ 3/2	$^4T_2\zeta$ 1/2	$^4T_2\xi$ −1/2	$^4T_2\eta$ −1/2	$^4T_2\zeta$ −3/2
$^2T_2\zeta$ 1/2	$-1/2$	$-i/2$	0	$-1/2\sqrt{3}$	$i/2\sqrt{3}$	0
$^2T_2\xi$ −1/2	0	0	$1/2\sqrt{3}$	0	$-i/\sqrt{3}$	1/2
$^2T_2\eta$ −1/2	0	0	$i/2\sqrt{3}$	$i/\sqrt{3}$	0	$-i/2$
$^4T_2\xi$ 3/2	0	$i/4$	$-1/4\sqrt{3}$	0	0	0
$^4T_2\eta$ 3/2	$-i/4$	0	$i/4\sqrt{3}$	0	0	0
$^4T_2\zeta$ 1/2	$-1/4\sqrt{3}$	$-i/4\sqrt{3}$	0	1/6	$-i/6$	0
$^4T_2\xi$ −1/2	0	0	1/6	0	$-i/12$	$-1/4\sqrt{3}$
$^4T_2\eta$ −1/2	0	0	$i/6$	$i/12$	0	$i/4\sqrt{3}$
$^4T_2\zeta$ −3/2	0	0	0	$-1/4\sqrt{3}$	$-i/4\sqrt{3}$	0

	$^2T_2\zeta$ 1/2	$^2T_2\xi$ −1/2	$^2T_2\eta$ −1/2
$^2T_2\zeta$ 1/2	0	−1/2	$i/2$
$^2T_2\xi$ −1/2	−1/2	0	$i/2$
$^2T_2\eta$ −1/2	$-i/2$	$-i/2$	0

for high spin ferric compounds are predominantly $^6A_1$ in character but contain excited doublet and quartet character as well. The eigenvectors were used to calculate Zeeman energies and hence g_x, g_y and g_z values within each of the three Kramers doublets. Since the operators L_x+2S_x and L_y+2S_y mix the $|E_{1/2}\alpha\rangle$ and $|E_{1/2}\beta\rangle$ time-reversal pairs in D_2' symmetry, the full 36×36 basis set was used in this calculation. The expressions for g values in terms of matrix elements of the basis states follow. (Notations are given in Table 2.)

$$\begin{aligned} g_z = {} & 2(5A^*A + B^*B - 3C^*C) + 2(J^*J - H^*H + 3M^*M - K^*K + O^*O - P^*P \\ & - 3R^*R + 3N^*N - L^*L + F^*F - 3I^*I + 3D^*D - G^*G - Q^*Q + 3E^*E) \\ & - i[-2(K^*L - L^*K) - (N^*M - M^*N) - (Q^*P - P^*Q) - (E^*D - D^*E) \\ & - (H^*G - G^*H) - \sqrt{3}\{-(D^*N - N^*D) - (E^*M - M^*E) - (H^*P - P^*H) \\ & - (G^*Q - Q^*G)\}] \end{aligned} \tag{8a}$$

$$\begin{aligned} g_x = {} & 2\sqrt{U^*U} \text{ where} \\ U = {} & 2[\sqrt{5}AC + \sqrt{8}BC + (3/2)B^2] + J^2 - K^2 - L^2 \\ & + 2[P^2 + Q^2 - O^2 + G^2 + H^2 - F^2] + 2\sqrt{3}(-OR + MP + NQ + DG \\ & - FI + EH) \\ & - i[NR + OQ + EI + FH + 2JL - \sqrt{3}(IN - HO + FQ - ER)] \end{aligned} \tag{8b}$$

$$g_y = 2\sqrt{W^* W} \text{ where}$$

$$W = 2[-\sqrt{5}AC + \sqrt{8}BC - (3/2)B^2] - K^2 - L^2 - J^2 + 2[P^2 + Q^2 + O^2 + G^2 + H^2 + F^2]$$
$$+ (-2JK - MR - OP - DI - FG) + 2\sqrt{3}(-OR - MP - NQ - FI - DG - EH)$$
$$-\sqrt{3}[IM - GO + FP - DR] \tag{8c}$$

Ground state spin-mixing (S and M_S) as reflected in the eigenvectors, g values and zero-field splittings is determined by the crystal field strength and the extent of axial and rhombic distortion. In the present scheme, calculations can be carried out in the high spin, low spin and intermediate spin as well as crossover regions.

Table 2. Time-reversal (KP) transformation properties of the basis state coefficients (complex conjugation is represented by *)

$A\Phi_1(^6A_1\ 5/2)$	$\xrightarrow{KP} A^*(^6A_1\ -5/2)$
$B\Phi_2(^6A_1\ 1/2)$	$\longrightarrow B^*(^6A_1\ -1/2)$
$C\Phi_3(^6A_1\ -3/2)$	$\longrightarrow C^*(^6A_1\ 3/2)$
$D\Phi_4(^4T_1x\ 3/2)$	$\longrightarrow D^*(^4T_1x\ -3/2)$
$E\Phi_5(^4T_1y\ 3/2)$	$\longrightarrow E^*(^4T_1y\ -3/2)$
$F\Phi_6(^4T_1z\ 1/2)$	$\longrightarrow -F^*(^4T_1z\ -1/2)$
$G\Phi_7(^4T_1x\ -1/2)$	$\longrightarrow G^*(^4T_1x\ 1/2)$
$H\Phi_8(^4T_1y\ -1/2)$	$\longrightarrow H^*(^4T_1y\ 1/2)$
$J\Phi_9(^4T_1z\ -3/2)$	$\longrightarrow -I^*(^4T_1z\ 3/2)$
$J\Phi_{10}(^2T_2\zeta\ 1/2)$	$\longrightarrow J^*(^4T_1\zeta\ -1/2)$
$K\Phi_{11}(^2T_2\xi\ -1/2)$	$\longrightarrow -K^*(^2T_2\xi\ 1/2)$
$L\Phi_{12}(^2T_2\eta\ -1/2)$	$\longrightarrow -L^*(^2T_2\eta\ 1/2)$
$M\Phi_{13}(^4T_2\xi\ 3/2)$	$\longrightarrow M^*(^4T_2\xi\ -3/2)$
$N\Phi_{14}(^4T_2\eta\ 3/2)$	$\longrightarrow N^*(^4T_2\eta\ -3/2)$
$O\Phi_{15}(^4T_2\zeta\ 1/2)$	$\longrightarrow -O^*(^4T_2\zeta\ -1/2)$
$P\Phi_{16}(^4T_2\xi\ -1/2)$	$\longrightarrow P^*(^4T_2\xi\ 1/2)$
$Q\Phi_{17}(^4T_2\eta\ -1/2)$	$\longrightarrow Q^*(^4T_2\eta\ 1/2)$
$R\Phi_{18}(^4T_2\zeta\ -3/2)$	$\longrightarrow -R^*(^4T_2\zeta\ 3/2)$

For tetragonal high spin ferric porphyrins, it has been shown that the three lowest Kramers doublets of the $^6A_1$ state are essentially distinct, i.e. M_S is substantially pure for each doublet [2]. However, as the axial bonding strength (C' and U') and/or the cubic crystal field component (Δ_{Oh}) become stronger, spin-mixing of excited quartet or doublet character into the ground state occurs. In contrast, the effect of increasing rhombicity is to mix M_S values within the $^6A_1$ manifold. Rhombicity mixes $|^6A_1 \pm \frac{1}{2}\rangle$ character into both higher Kramers doublets and enhances the probability of observing EPR transitions within them.

The rhombic splitting of the ^4T_1x and ^4T_1y states is to first order a function solely of the fourth order crystal field coefficient, A_{42} (See Fig. 2 and Eqs. (6) and (7)). The second order rhombic crystal field parameter, A_{22}, influences the $^4T_1$ term splitting and hence anisotropy of g values through rhombic and tetragonal crystal field mixing of the $^4T_2$ and $^4T_1$ terms (Eq. (7)).

The energy matrix contains 8 parameters: B, C, ζ, A_{42}, A_{22}, Δ_{Oh}, C' and U'. The Racah parameters, B and C, and the spin-orbit parameter, ζ are set at their free ion values ($B=1100\ cm^{-1}$, $C=3750\ cm^{-1}$, $\zeta=420\ cm^{-1}$), and the five crystal field parameters are varied systematically to fit the observed g values and zero-field splittings.

3. Fitting to Observed Zero-Field Splitting and g Values

Term energy assignments and self-consistency within the rhombic crystal field model in high spin ferric heme compounds imply that limits be placed on the variation of the five crystal field parameters, Δ_{Oh}, C', U', A_{22} and A_{42} relative to one another and to the Racah and spin-orbit interaction parameters chosen. We constrain the one-electron orbital splittings of high spin ferric heme compounds as follows [10, 11]

$$d_{yz}, d_{xz} > d_{xy} \qquad (9)$$
$$d_{x^2-y^2} > d_{z^2}$$

and

$$\delta' > \delta > 0 \qquad (10)$$

Then from (5), (9) and (10) it follows that

$$\Delta_{Oh} > C' > 0 \qquad (11)$$

and

$$0 < U' < \tfrac{4}{3}C' \qquad (12)$$

The first of the constraints (9) may be over-restrictive in some low-spin systems with a strong $d\pi$–$p\pi^*$ interaction. These restrictions of parameters are in agreement with the point charge model which implies that C' and U' must always have the same sign in a complex since they both represent the difference between in-plane and axial bonding strength [2]. Furthermore, U' and C' decrease together as the axial field increases relative to the in-plane field. If we define F as the ratio of C' to U', it gives the ratio of fourth order to second order tetragonal distortion parameters. Clearly, F is always positive. The magnitude of F is a measure of the relative magnitudes of the t_{2g} and e_g tetragonal splittings δ and δ', respectively [2]. Since $U' \leqslant \frac{4}{3}C'$, it follows that $E(^2T_2\zeta) > E(^2T_2\xi, \eta)$, and $F > 0.75$. When F is at its lower limit, $\delta' \gg \delta$. As $F \to \infty$, $\delta' \approx \delta$. In the tetragonal limit, g values and zero-splittings are relatively insensitive to wide variation of the value of F (all other parameters held fixed). However, for the case of rhombic distortion, when the $^4T_2$ state is included in the calculation, g value anisotropy becomes quite sensitive to variations in F. For calculations using the large basis set with a given set of parameters, as F increases, g value anisotropy decreases; however, zero-field splittings are only slightly more sensitive to variation of F in rhombic symmetry than they are in the tetragonal limit.

Table 3. g values and zero-field splittings calculated for various rhombicities with the 12×12 and 18×18 matrix representations with $\Delta_{Oh}=27437\ cm^{-1}$, $C'=4660\ cm^{-1}$ and $F=1.32$

	A_{22}	A_{42}	$g_x(1)$	$g_y(1)$	$g_z(1)$	$g_x(2)$	$g_y(2)$	$g_z(2)$	ΔE_1	ΔE_2
12×12	91.22	3231.4	4.36	7.46	1.85	1.58	1.51	5.82	6.79	13.43
18×18			3.93	7.81	1.77	2.00	1.87	5.76	6.84	13.17
12×12	91.22	2225	4.87	7.04	1.93	1.09	1.07	5.90	6.66	13.52
18×18			4.56	7.31	1.89	1.40	1.35	5.88	6.61	13.26
12×12	91.22	1660	5.16	6.79	1.96	0.82	0.81	5.94	6.61	13.56
18×18			4.93	7.00	1.94	1.04	1.03	5.93	6.52	13.30
12×12	91.22	930	5.53	6.45	1.99	0.46	0.48	5.96	6.56	13.59
18×18			5.40	6.57	1.98	0.58	0.59	5.98	6.44	13.33
12×12	91.22	445	5.77	6.21	1.998	0.21	0.23	5.97	6.55	13.60
18×18			5.72	6.27	1.996	0.27	0.29	5.997	6.41	13.34
12×12	0	0	5.99	5.99	2.00	0.014	0.014	5.98	6.54	13.61
18×18			5.99	5.99	2.00	0.014	0.014	5.98	6.54	13.61

The larger the magnitude of Δ_{Oh}, the lower the ^4T_1z state lies and the more strongly it interacts with the ground state (see Fig. 2 and Eq. (7)). As we have discussed above, the $^4T_1$ state and its splittings in tetragonal and rhombic crystal fields are directly reflected in the zero-field splitting and in anisotropy of g values. Using a second order spin-orbit perturbation of the ground state by the $^4T_1$ state, the quadratic spin Hamiltonian parameters D and E can be related to energy differences E_z, E_x and E_y between the $^6A_1$ term and the ^4T_1z, ^4T_1x and ^4T_1y excited states, respectively [12].

$$D=\frac{\zeta^2}{10}\left(\frac{2}{E_z}-\frac{1}{E_x}-\frac{1}{E_y}\right)$$
$$E=\frac{\zeta^2}{10}\left(\frac{1}{E_x}-\frac{1}{E_y}\right) \tag{13}$$

The expansions of D and E in terms of $^4T_1$ energy levels are good approximations for the limited basis set (which excludes $^4T_2$, see [5]). Since $C'>0$, the ^4T_1z level lies below the average energy of ^4T_1x and ^4T_1y (Fig. 2) and therefore $D>0$. Internal consistency is now assured amongst the magnitudes and signs of C', U', δ, δ' and D. Since to first order the rhombic splitting of the ^4T_1x and ^4T_1y levels is a function of A_{42} alone, reversing the sign of A_{42} when $A_{22}=0$ merely interchanges g_x and g_y and leaves zero-field splitting invariant. When A_{42} is positive, g_x is smaller than g_y. When $E(^4T_1x)<E(^4T_1y)$, then $E>0$.

The second order crystal field parameter, A_{22} can be positive or negative. When the $^4T_2$ state is included in the energy matrix, the g values are quite sensitive to variation of A_{22} (when all other parameters are fixed). However, within the restricted basis

Table 4. Comparison of 12×12 and 18×18 matrix representations to calculate g values for model species I ($TPPH_2(FeX)$) using five sets of crystal field values predicted by a perturbation analysis of the limited 12×12 basis set [5]

	$g_x(1)$	$g_y(1)$	$g_z(1)$	$g_x(2)$	$g_y(2)$	$g_z(2)$	ΔE_1 (cm^{-1})	ΔE_2 (cm^{-1})
Experimental	3.983	7.797	1.783	1.978	1.811			
Calculated (12×12)								
I	3.939	7.804	1.775	1.995	1.866	5.760	6.724	12.83
II	3.957	7.779	1.779	1.978	1.851	5.765	6.681	12.81
III	3.915	7.816	1.769	2.012	1.883	5.755	6.757	13.17
IV	3.896	7.829	1.764	2.030	1.898	5.750	6.798	13.19
V	3.927	7.810	1.772	2.003	1.874	5.758	6.739	12.99
Calculated (18×18)								
I	3.137	8.386	1.572	2.732	2.501	5.537	7.564	13.28
II	3.507	8.125	1.674	2.395	2.212	5.649	8.270	15.19
III	3.633	8.029	1.704	2.275	2.111	5.684	7.043	13.33
IV	3.584	8.063	1.691	2.319	2.151	5.670	6.909	12.97
V	3.486	8.139	1.668	2.413	2.229	5.643	7.176	13.23

Key	Δ_{Oh} (cm^{-1})	C' (cm^{-1})	F	μ' (cm^{-1})	$-\mu$ (cm^{-1})	A_{22} (cm^{-1})	A_{42} (cm^{-1})
I	27208.0	4858.3	1.0833	5353	1380	−7240	3650
II	27194.0	4854.9	2.7257	7727	3433	−11995	3653
III	28585.5	4108.6	7.5763	2363	−504	−2160	2859
IV	27589.0	4133.1	1.7522	883	−1802	760	2877
V	27421.2	4409.7	2.3723	3328	53	−3782	3171

set ($^6A_1$, $^4T_1$ and $^2T_2$), A_{22} can be varied widely with only slight changes in anisotropy of g values. In the full 18×18 perturbation matrix, when the rhombic parameter A_{22} increases alone, ΔE_1 and ΔE_2 both decrease. However, when A_{42} increases, ΔE_1 increases and ΔE_2 decreases (Fig. 2, Table 5), the sign of μ can be positive or negative depending on the distortion axis of the molecule. A one-electron picture does not restrict the sign of μ' since it enters into the rhombic mixing of d_{z^2} and $d_{x^2-y^2}$ as a squared quantity.

An approximate fit of Δ_{Oh}, C' and A_{42} to the zero-field splitting and g values, can be obtained from the spin Hamiltonian parameters, D and E if known separately. Using Eqs. (7) and (13) we can obtain a relationship among C', A_{42} and Δ_{Oh} reflecting the order of perturbation used in Eq. (13). We can restrict F and A_{22} arbitrarily in this approximation since these parameters affect ground state properties only through states above the $^4T_1$ state. Using Δ_{Oh}, C' and A_{42} chosen as described above, and arbitrary F and A_{22}, we can perform calculations of g values and zero-field splitting energies. To first order, we set $A_{22}=0$ and $F>0.75$. A_{22} and F were then adjusted for a higher order fit.

When B, C and ζ are set at their free ion values (see Section 2), Δ_{Oh} for high spin heme proteins falls between 26000 cm^{-1} and 31000 cm^{-1} [2]. By using one value

Table 5. Calculation of g values and zero-field splittings for model compounds I-XVII. ($\Delta_{Oh} = 27437$ cm^{-1}, $C' = 4660$ cm^{-1}, $F = 1.32$, $A_{22} = -365$ cm^{-1}, A_{42} varies). For details of this model system see Ref. [5]

Model compound species	A_{42}	ΔE_1	ΔE_2	$g_x(1)$	$g_y(1)$	$g_z(1)$	$g_x(2)$	$g_y(2)$	$g_z(2)$	
I	3155	6.819	13.17	3.978	7.771	1.782	1.956	1.832	5.768	Calc.
				3.983	7.796	1.783	1.979	1.811		Exp.
II	2550	6.674	13.23	4.354	7.475	1.854	1.597	1.521	5.846	Calc.
				4.354	7.499	1.855	1.628	1.988		Exp.
III	2540	6.672	13.23	4.360	7.470	1.855	1.591	1.516	5.847	Calc.
				4.360	7.486	1.855	1.620	1.476		Exp.
IV	2460	6.655	13.23	4.411	7.429	1.864	1.542	1.473	5.856	Calc.
				4.410	7.446	1.864	1.573	1.441		Exp.
V	2225	6.608	13.26	4.560	7.306	1.888	1.398	1.345	5.882	Calc.
				4.556	7.335	1.889	1.447	1.298		Exp.
VI	2205	6.604	13.26	4.573	7.295	1.889	1.385	1.334	5.884	Calc.
				4.575	7.328	1.890	1.436	1.282		Exp.
VII	1800	6.536	13.29	4.834	7.074	1.926	1.132	1.107	5.922	Calc.
				4.831	7.103	1.927	1.190	1.050		Exp.
VIII	1770	6.531	13.29	4.853	7.058	1.928	1.113	1.090	5.925	Calc.
				4.858	7.077	1.930	1.161	1.018		Exp.
IX	1660	6.515	13.30	4.925	6.996	1.937	1.044	1.026	5.934	Calc.
				4.936	7.009	1.940	1.100	0.930		Exp.
X	1365	6.477	13.31	5.117	6.827	1.957				Calc.
				5.118	6.851	1.960				Exp.
XI	1200	6.459	13.32	5.224	6.730	1.967				Calc.
				5.294	6.697	1.976				Exp.
XII	930	6.435	13.33	5.400	6.569	1.980				Calc.
				5.406	6.590	1.980				Exp.
XIII	580	6.412	13.34	5.628	6.355	1.993				Calc.
				5.637	6.366	2.00				Exp.
XIV	460	6.407	13.34	5.705	6.281	1.996				Calc.
				5.73	6.289	2.00				Exp.
XV	445	6.406	13.34	5.715	6.271	1.996				Calc.
				5.729	6.280	2.00				Exp.
XVI	385	6.404	13.35	5.734	6.234	1.997				Calc.
				5.796	6.235	2.00				Exp.
XVII	350	6.403	13.35	5.776	6.212	1.998				Calc.
				5.798	6.232	2.00				Exp.

of D and E and varying Δ_{Oh}, C' and A_{42} together in accordance with Eqs. (7) and (13), a wide range of crystal field parameters may be found which give calculated g values and zero-field splitting energies which are almost constant. Physically, this implies that many different molecular arrangements or mechanisms of rhombicity are consistent with the same set of lowest Kramers doublet g values and zero-field splittings. Fig. 3 gives the three-fold variation of A_{42}, C' and Δ_{Oh} used in fitting g values for rhombic ferric species I with $E/D = 0.08234$ and $D = 3.219$

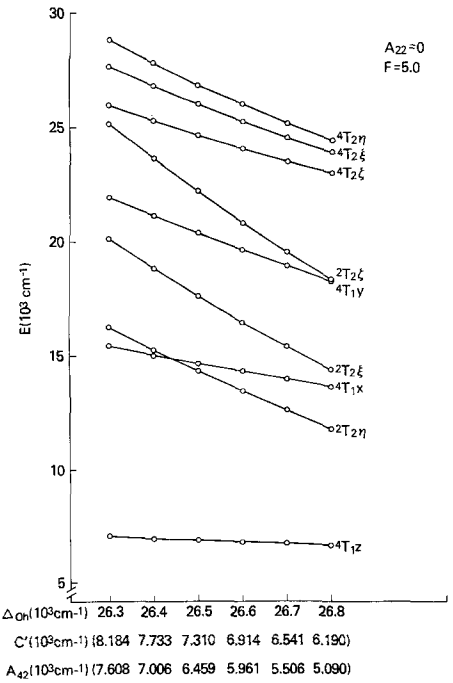

Fig. 3. Term energies with crystal field mixing (and no spin-orbit interaction) corresponding to the set of g values and zero-field splittings ($\Delta E_1 = 7.06\ \text{cm}^{-1}$, $\Delta E_2 = 12.9\ \text{cm}^{-1}$, $g_x(1) = 3.63$, $g_y(1) = 8.04$, $g_z(1) = 1.70$) while Δ_{Oh}, C' and A_{42} vary simultaneously. The abscissa is true only for Δ_{Oh}. The associated values of C' and A_{42} are given in parentheses. Eigenvector designations correspond to the dominant state after crystal field mixing

([5], Table 2). The range of Δ_{Oh} was 500 cm^{-1}. F was set at 5.0 and A_{22} was zero. As we increase Δ_{Oh} and decrease C' and A_{42} simultaneously, the energy of the $^4T_1$ states decrease and at the same time the splitting within the $^4T_1$ term decreases. In heme compounds, if Δ_{Oh} is increasing while C' decreases, then axial bonding strength is increasing [2]. When the smaller basis set (which excludes $^4T_2$) was used, the calculated values fall within 1% of $\Delta E_1 = 6.83$, $\Delta E_2 = 12.8$, $g_x(1) = 3.96$, $g_y(1) = 7.79$, $g_z(1) = 1.78$, $g_x(2) = 1.99$ and $g_y(2) = 1.85$. $g_i(1)$ and $g_i(2)$ refer to the g values arising from the lowest and middle Kramers doublets, respectively. The agreement of g values with experiment (Table 7) demonstrates the validity of the approximation used in Eq. (13) for the smaller basis set. Using the larger basis set, values were constant within 2% around $\Delta E_1 = 7.06$, $\Delta E_2 = 12.9$, $g_x(1) = 3.63$, $g_y(1) = 8.04$, $g_z(1) = 1.70$, $g_x(2) = 2.30$ and $g_y(2) = 2.11$. As we can see, the g values calculated with the larger basis set are more rhombic than those calculated within the smaller basis for the same set of crystal field parameters.

If E and D are known separately, and if sufficient data are available, the range of crystal field parameters may be restricted further by analysis of the quartic terms of the spin Hamiltonian. In the case of the mixed crystal rhombic system mentioned above, five g values (three for the lowest Kramers doublet and g_x and g_y for the middle Kramers doublet) were measured [6]. The full spin Hamiltonian including quartic as well as quadratic terms [5], was analyzed.

Note that if the algorithm described above is not used to vary Δ_{Oh}, C' and A_{42} together and instead parameters are varied one at a time, the calculated g values and zero-field splitting energies diverge significantly when each parameter is

Table 6. Coefficients of the $^6A_1$ ground state for the three lowest Kramers doublets of model compounds I-XVII (parameters are the same as those used in Table 5)

Model compound species	A_{42}	Lowest Kramer's doublet			Middle Kramer's doublet			Upper Kramer's doublet		
		$^6A_1 \pm 1/2$	$^6A_1 \mp 3/2$	$^6A_1 \pm 5/2$	$^6A_1 \pm 1/2$	$^6A_1 \mp 3/2$	$^6A_1 \pm 5/2$	$^6A_1 \pm 1/2$	$^6A_1 \mp 3/2$	$^6A_1 \pm 5/2$
I	3155	0.9812	0.1699	0.0416	0.1695	0.9828	0.0126	0.0432	0.0054	0.9980
II	2550	0.9863	0.1390	0.0337	0.1389	0.9876	0.0098	0.0347	0.0041	0.9984
III	2540	0.9863	0.1385	0.0336	0.1383	0.9877	0.0088	0.0345	0.0040	0.9984
IV	2460	0.9870	0.1344	0.0326	0.1342	0.9883	0.0084	0.0334	0.0039	0.9984
V	2225	0.9887	0.1220	0.0295	0.1219	0.9899	0.0071	0.0302	0.0035	0.9985
VI	2205	0.9889	0.1210	0.0292	0.1208	0.9900	0.0070	0.0299	0.0034	0.9985
VII	1800	0.9914	0.0993	0.0239	0.0992	0.0024	0.0052	0.0243	0.0028	0.9987
VIII	1770	0.9916	0.0977	0.0235	0.0976	0.9926	0.0051	0.0239	0.0028	0.9987
IX	1660	0.9922	0.0917	0.0221	0.0917	0.9932	0.0047	0.0224	0.0027	0.9987
X	1365	0.9936	0.0756	0.0181	0.0756	0.9945	0.0037	0.0184	0.0023	0.9988
XI	1200	0.9943	0.0666	0.0159	0.0665	0.9952	0.0032	0.0161	0.0022	0.9989
XII	930	0.9950	0.0516	0.0123	0.0516	0.9961	0.0026	0.0125	0.0020	0.9989
XIII	580	0.9961	0.0321	0.0077	0.0321	0.9969	0.0020	0.0077	0.0018	0.9990
XIV	460	0.9963	0.0254	0.0060	0.0254	0.9971	0.0019	0.0061	0.0017	0.9990
XV	445	0.9964	0.0245	0.0058	0.0245	0.9971	0.0019	0.0059	0.0017	0.9990
XVI	385	0.9964	0.0212	0.0050	0.0212	0.9972	0.0018	0.0051	0.0017	0.9990
XVII	350	0.9965	0.0192	0.0046	0.0192	0.9972	0.0018	0.0046	0.0017	0.9990

Table 7. Crystal field parameters, g values and zero-field energies for some high spin ferric heme compounds of different rhombicities

	Δ_{Oh} (cm^{-1})	C' (cm^{-1})	F	μ' (cm^{-1})	μ (cm^{-1})	A_{42} (cm^{-1})	A^{22} (cm^{-1})	ΔE_1	ΔE_2	$g_x(1)$	$g_y(1)$	$g_z(1)$	$g_x(2)$	$g_y(2)$	$g_z(2)$
Model species I (Fe^{+3}TPP) in $TPPH_2$	27437	4660	1.32	1364.8	1199.9	2670	−365	6.87	13.14	3.96	7.79	1.78	1.97	1.85	5.76
							exp [6]:	–	–	3.98	7.79	1.78	1.98	1.81	–
							$E/D=0.0823$	$D=3.219$							
P-450_{cam}	27700	6095	1.32	1673	2116	3996.2	178.8	8.1	15.4	3.95	7.79	1.78	1.99	1.85	5.76
							exp:	8.1[2]	–	3.95[1]	7.81[1]	1.78[1]	–	–	–
							$E/D=0.087$[2]	$D=3.8$[2]							
P-450, Rabbit liver microsome	27850	6034	1.32	2550	1654	4329.7	−1252.8	8.6	15.95	3.74	7.95	1.73	2.18	2.02	5.71
							exp:	8.6[2]	–	3.74[1]	7.96[1]	1.73[1]	–	–	–
							$E/D=0.095$[2]	$D=3.95$[2]							
Metmyoglobin fluoride	29400	8212	1.32	207.5	169.4	391	−68	12.9	26.4	5.87	6.09	2.00	0.106	0.115	6.00
							exp [4]:	–	–	5.87	6.05	2.00	–	–	–
							$E/D=0.0038$	$D=6.5$[3]							
Metmyoglobin	30550	8605	1.32	264.9	216	499	−87	19	39	5.86	6.08	2.00	0.106	0.114	6.00
							exp [4]:	–	–	5.85	5.98	2.00	–	–	–
							$E/D=0.0025$	$D=10$[3]							

[1] Data measured in this laboratory.

[2] Peisach, J., Blumberg, W. E.: Proc. Nat. Acad. Sci., USA **67**, 172 (1970).

[3] Tasaki, A., Otsuka, J., Kotani, M.: Biochim. Biophys. Acta **140**, 284 (1967).

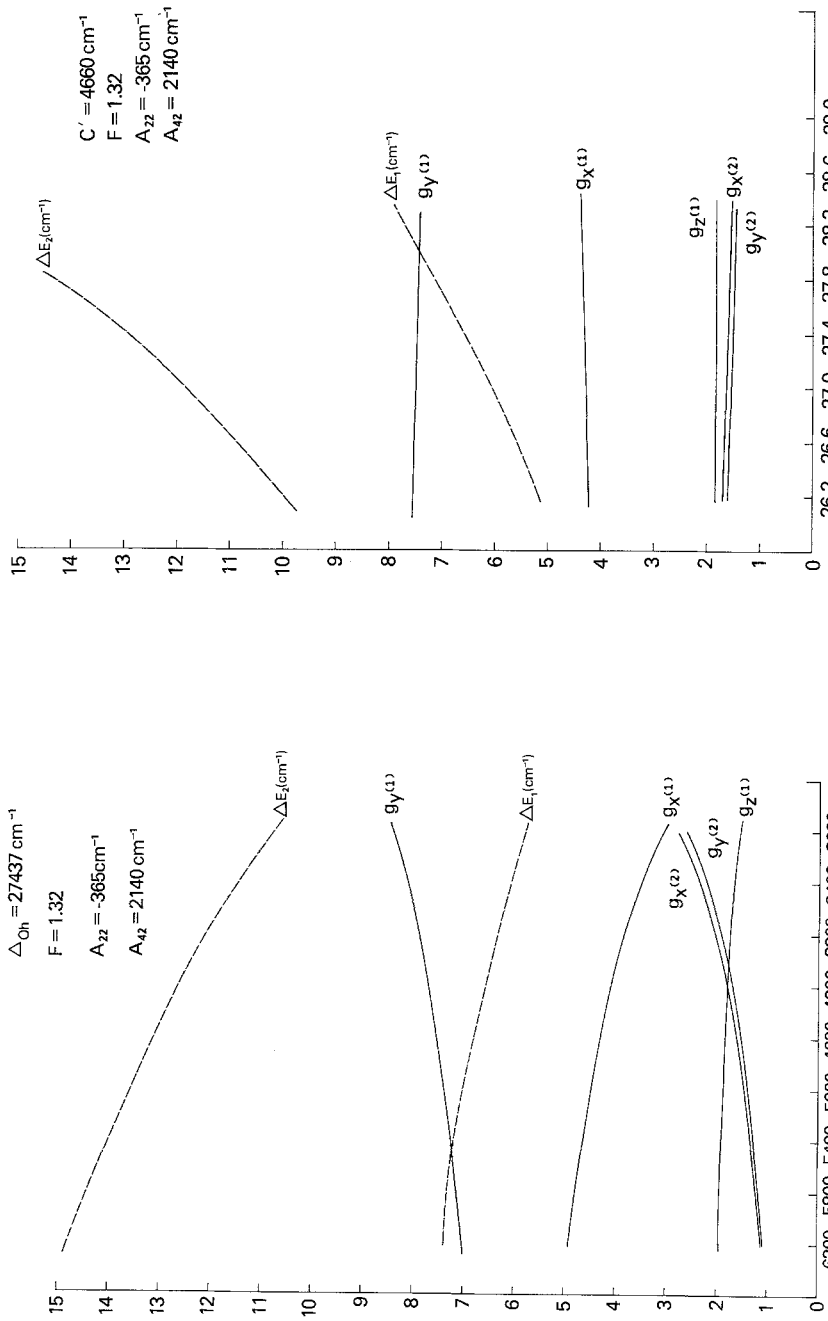

Fig. 4. Change of zero-field splittings and rhombicity of g values with variation of (a) tetragonal parameter C', and (b) octahedral parameter (Δ_{Oh})

varied by a few wave numbers (Figs. 4, 5). For tetragonal compounds in which D is known, a simplified algorithm can be used to fit g values and ΔE_1 with a total of three parameters. Thus we were able to fit g values and zero-field splittings [13] for tetragonal ferric porphyrins in several ways.

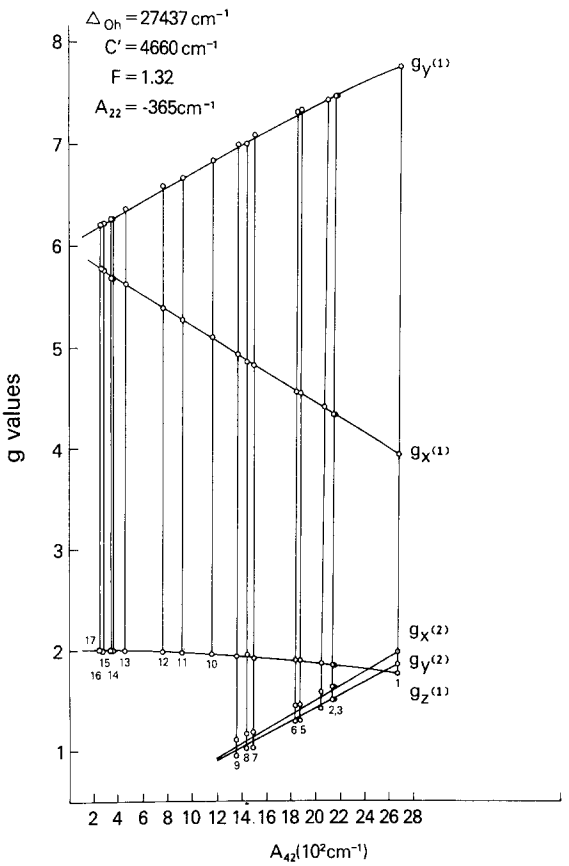

Fig. 5. Calculated (solid lines) and observed (circles) g values for the lowest and middle Kramers doublets of seventeen model compounds of different rhombicities

4. Results

In order to demonstrate the effect of the extra excited $^4T_2$ state on $^6A_1$ ground state properties in rhombically distorted ferric porphyrins, we have calculated g values and zero-field splittings for mixed crystal model compounds of varying rhombicities using the full basis set $^6A_1$, $^4T_1$, $^2T_2$, $^4T_2$ (18×18 matrix representation) as well as a more limited basis excluding the $^4T_2$ state (12×12 matrix representation). In the tetragonal limit with both rhombic parameters, A_{22} and A_{42} equal to zero, the lowest Kramers doublet g values are coincident for the two representations. As the value of A_{42} increases (Table 3), the differences between g_x and g_y calculated by the two schemes increases. Consideration of $g_x(1)$ and $g_y(1)$ shows that calculations using the full basis set (18×18) yield g values that are clearly more anisotropic for each parameter value than those calculated with the 12×12 representation.

In another comparison of effective rhombicity due to the extra $^4T_2$ term, g values were calculated (Table 4) for the mixed crystalline model compound species I using five sets of crystal field parameters predicted by the spin Hamiltonian treatment ([15] Table 2). The effect of variation of A_{22}, A_{42} and F is amplified by inclusion of the $^4T_2$ term and transmitted to the $^4T_1$ term to cause wider scattering in calculated g values, since the tetragonal and rhombic crystal field matrix elements mix the $^4T_1$ state only with the $^4T_2$ state.

A comparison of excited state term energies was made using both basis sets with one set of crystal field parameters, namely $\Delta_{Oh}=27437\ cm^{-1}$, $C'=4600\ cm^{-1}$, $F=1.32$, $A_{22}=-365\ cm^{-1}$ and $A_{42}=2670\ cm^{-1}$. The $^4T_1x, y$ energy difference increased from $2350\ cm^{-1}$ for the 12×12 representation to $2983\ cm^{-1}$ for the 18×18 representation (including the $^4T_2$ state). The g values demonstrate greater rhombic distortion as well.

In Fig. 3 are the term energies which correspond to the surface in crystal field parameter space for $D=3.219$ and $E=0.2651$ (See [5] Table 2, mixed crystalline species I). For this surface, g values and zero-field energies are essentially constant. The term energies range from one extreme in which the $^2T_2$ and $^4T_1$ levels alternate to another in which the $^2T_2$ levels have moved down towards the ground state. Over the range of parameters, the crystal field strength is increasing toward the low spin limit. This corresponds to movement of the ferric ion towards the porphyrin plane as the tetragonal parameter C' decreases (when axial bonding strength increases, C' decreases). Note that as C' decreases, g values are unchanged as long as the rhombic parameter, A_{42} decreases. Although a wide variation of term and one-electron energy splittings can give rise to the same ground state properties, the surface is characterized uniquely by E and D.

To see the effect on one-electron rhombic splitting and calculated g values when $A_{42}=0$, we let Δ_{Oh} $27437\ cm^{-1}$, $C'=4660\ cm^{-1}$, $F=1.32$ and $A_{22}=9115\ cm^{-1}$. This choice of Δ_{Oh}, C' and F is the one used to fit the g values of the seventeen mixed crystalline rhombic species. $TPPH_2(FeX)$ (See Tables 5 and 6). Our initial restrictions (9) and (10) place an upper bound of $9115\ cm^{-1}$ on the size of A_{22} when A_{42} is zero; when $A_{22}>9115\ cm^{-1}$ and $A_{42}=0$, $d_{yz}<d_{xy}$ (Fig. 1) which contradicts our initial restrictions. The one-electron rhombic splittings, μ and μ', have larger magnitudes than they do in fitting mixed crystal species I, yet the anisotropy in the calculated g values is much smaller, i.e. $g_x(1)=5.54$, $g_y(1)=6.43$ and $g_z(1)=1.99$. When $A_{42}=0$, the splitting of the ^4T_1x and ^4T_1y states is due only to their interaction with higher lying states and the difference between $g_x(1)$ and $g_y(1)$ is small.

Rhombic distortion mixes M_S values within the $^6A_1$ ground state. Table 6 gives the coefficients of the three lowest Kramers doublet eigenvectors calculated by the crystal field formalism for model species I through XVII. The g values for these compounds were fitted by variation of A_{42} alone (Fig. 5, Table 5). The extent of mixing of $|^6A_1\pm\frac{3}{2}\rangle$ and $|^6A_1\pm\frac{5}{2}\rangle$ character within the lowest Kramers doublet varies from 0.03% and 0.002%, respectively, for species XVII to 2.9% and 0.18%, respectively, for species I. Rhombic distortion, however, does not appreciably change the extent of spin mixing of quartet and doublet character into the ground

sextet state for the compounds studied. (Quartet and doublet character in the lowest Kramers doublet is 0.667% for species XVII and 0.665% for species I). As rhombicity increases, zero-field splitting, ΔE_1 increases from 6.4 to 6.9 while ΔE_2 decreases from 13.3 to 13.1 from species XVII to I.

Although to first order in a magnetic field, the observation of EPR transitions within the second and third Kramers doublet is forbidden, rhombicity, by mixing $|^6A_1 \pm \frac{1}{2}\rangle$ character into these states, enhances the probability of observing EPR transitions in the middle and upper Kramers doublets [14]. To higher order, the perpendicular component of the magnetic field can also mix $|^6A_1 \pm \frac{1}{2}\rangle$ character with $|^6A_1 \mp \frac{3}{2}\rangle$. This higher order Zeeman mixing becomes increasingly significant as zero-field splitting decreases and magnetic field increases. Rhombicity can be expected to enhance the non-linear magnetic field effect by mixing $|^6A_1 \pm \frac{1}{2}\rangle$ character into the middle and upper Kramers doublets. Deviations of calculated from observed g values (Table 5, Fig. 5) for the middle Kramers doublet are caused by the third order Zeeman effect [5].

Crystal field parameters, g values and zero-field splittings are displayed in Table 7 for metmyoglobin, metmyoglobin fluoride, cytochrome P-450$_{cam}$, mammalian (rabbit liver microsomal) cytochrome P-450 and mixed crystalline model compound ($TPPH_2$(FeX)) species I. The latter three compounds fall well within the high spin limits for ferric ion. Metmyoglobin and metmyoglobin fluoride are close to the crossover point to the low spin state and thus have increased mixing of quartet and doublet character into their ground state wave functions. The rhombicity of P-450$_{cam}$ is comparable to that of mixed crystalline model species I ($TPPH_2$(FeX)), and metmyoglobin and its fluoride derivative are less rhombic than the least rhombic mixed crystalline model compound.

5. Conclusions

For high spin ferric ion in rhombic symmetry, we have used a crystal field model to relate term splittings of the $^4T_1$, $^2T_2$ and $^4T_2$ excited states to zero-field split energies and g values of the $^6A_1$ term. In this model five crystal field parameters were used, namely, one cubic parameter, two tetragonal parameters and second and fourth order rhombic parameters. In tetragonal symmetry with only three crystal field parameters, a simpler model including only the $^4T_1$ and $^2T_2$ excited states is adequate to relate term energies to g values and zero-field split energies. However, we have demonstrated the importance of the $^4T_2$ state in rhombic crystalline fields.

Knowledge of the quadratic spin Hamiltonian parameter E and D have been shown to be crucial in obtaining a surface in parameter space which gives almost constant zero-field split energies and g values. This surface corresponds to a variation of term splittings. For a compound which has intermediate crystal field strength with large rhombicity, such as the mixed crystalline model compound species I ($TPPH_2$(FeX)), the term splittings may range from one extreme in which the $^2T_2$ levels alternate with the $^4T_1$ levels to one in which the $^2T_2$ levels have moved

towards the ground state. In the latter case, the crystal field strength is increasing toward the low spin limit, corresponding to movement of the ferric ion towards the porphyrin plane. When sufficient data are available, e.g. g values from the middle as well as lowest Kramers doublets, the quartic spin Hamiltonian parameters are obtainable and the crystal field parameters corresponding to the g values can be defined.

The g values for seventeen mixed crystalline ferric species ($TPPH_2(FeX)$) of rhombicities varying from slightly rhombic (on the order of metmyoglobin) to highly rhombic (g values comparable to those of cytochrome P-450) have been calculated. As rhombicity increases, the extent of M_S mixing within the lowest Kramers doublets has been shown to increase.

Crystal field parameters have been compared in calculations of g values and zero-field split energies for metmyoglobin fluoride, metmyoglobin, cytochrome $P\text{-}450_{cam}$, mammalian (rabbit) cytochrome P-450, and mixed crystalline model compound species I ($TPPH_2(FeX)$). Zero-field splittings and g values for the lowest Kramers doublet were known for the first four heme compounds, as well as estimates of D and E. Further data such as knowledge of d-d transitions in ferric ions in tetragonal and rhombic symmetries would remove some of the ambiguity in choice of crystal field parameters. Although g values are available for many other heme proteins, zero-field splittings are not available and separate determinations of D and E have not yet been made. When only E/D is known, the calculation is extremely underdetermined.

Thus, as far as experimental knowledge for rhombic ferric complexes will allow, our model, a crystal field calculation including three excited states ($^4T_1$, $^2T_2$ and $^4T_2$), can account for ground state g values and zero-field split energies in relation to term splittings and crystal field parameters. These parameters can be related to one-electron splittings of ferric ion to give some insight into rhombic distortion of the environment.

References

1. Kotani, M.: Rev. Mod. Phys. **35**, 717 (1963)
2. Harris, G.: J. Chem. Phys. **48**, 2191 (1968); Theoret. Chim. Acta (Berl.) **10**, 119 (1968); Theoret. Chim. Acta (Berl.) **10**, 155 (1968)
3. Otsuka, J.: J. Phys. Soc. Japan **21**, 885 (1968)
4. Eicher, H.: Z. Naturforsch **30C**, 701 (1975)
5. Sato, M., Rispin, A. S., Kon, H.: Chem. Phys. **18**, 211 (1976)
6. Sato, M., Kon, H.: Chem. Phys. **12**, 199 (1976)
7. Griffiths, J. S.: The theory of transition metal ions. London: Cambridge University Press 1961; Griffiths, J. S.: The irreducible tensor method for molecular symmetry groups. Englewood Cliffs, N.J.: Prentice-Hall, Inc. 1962
8. Rispin, A. S.: Doctoral Thesis, Catholic University of America 1972
9. Sugano, S., Tanabe, Y., Kamimura, H.: Multiplets of transition-metal ions in crystals. New York, N.Y.: Acadedic Press 1970
10. George, P., Beetlestone, J., Griffith, J. S.: Rev. Mod. Phys. **36**, 441 (1964)

11. Zerner, M., Gouterman, M., Kobayashi, H.: Theoret. Chim. Acta (Berl.) **6**, 363 (1966)
12. Kotani, M., Watari, H.: Magnetic resonance in biological research, 75, Franconi, C. Ed. New York, N.Y.: Gordon and Breach Science Publishers 1971
13. Richards, P. L., Caughey, W. S., Eberspaecher, H., Feher, G., Malley, M.: J. Chem. Phys. **47**, 1187 (1967)
14. Weissbluth, M.: Hemoglobin cooperativity and electronic properties. New York, N.Y.: Springer-Verlag 1974

Received November 2, 1977/June 16, 1978